Supporting Information

Structural and mechanistic insights into bisphenols action provide guidelines for risk assessment and discovery of BPA substitutes

Vanessa Delfosse[a,b], Marina Grimaldi[c,d,e,f], Jean-Luc Pons[a,b], Abdelhay Boulahtouf[c,d,e,f], Albane le Maire[a,b], Vincent Cavailles[c,d,e,f], Gilles Labesse[a,b], William Bourguet[a,b] and Patrick Balaguer[c,d,e,f]

[a]INSERM U1054, Centre de Biochimie Structurale, 34090 Montpellier, France; [b]CNRS UMR5048, Universités Montpellier 1 & 2, 34090 Montpellier, France; [c]IRCM, Institut de Recherche en Cancérologie de Montpellier, 34298 Montpellier, France; [d]INSERM, U896, 34298 Montpellier, France; [e]Université Montpellier 1, 34298 Montpellier, France; [f]CRLC Val d'Aurelle Paul Lamarque, 34298 Montpellier, France.

William Bourguet: Phone: +(33) 4 67 41 7702
Fax: +(33) 4 67 41 7913
e-mail: bourguet@cbs.cnrs.fr

Patrick Balaguer: Phone: +(33) 4 67 61 2409
Fax: +(33) 4 67 61 37 87
e-mail: Patrick.Balaguer@montpellier.unicancer.fr

Materials and Methods

Ligands and peptides. BPA, BPC, BPAF and other bisphenols were purchased from Sigma Aldrich (Saint Quentin Fallavier, France). E_2 and OHT were kindly provided by Sanofi-Aventis (Gentilly, France). [^{3}H]-E_2 (41.3 Ci/mmol specific activity) was purchased from NEN Life Science Products (Paris, France). The fluorescein-RHKILHRLLQEGS peptide corresponding to the NR box 2-binding motif of SRC-1 was purchased from EZbiolab (Westfield, Indiana, USA).

Reporter cell lines and culture conditions. The stably transfected luciferase reporter MELN, HELN-ERα, -ERβ, -ΔAB-ERα and -ΔAB-ERβ cell lines have been already described (1). To characterize the bisphenol-induced AR and ERRγ activity, we expressed AR with ERα DNA binding domain and the ERRγ LBD fused to GAL4 DNA binding domain in HELN (HeLa ERE-luciferase) and HG5LN (HeLa GAL4REx5-luciferase). Luciferase, cell proliferation and whole-cell ER competitive binding assays have been performed as described in (1).

Transient transfection experiments. ERα WT and Y537S, ERβ, ΔAB-ERα and ΔAB-ERβ activity was monitored on ERE-βGlobin- and pS2-luciferase reporter constructs in HeLa cells. Transient transfection and luciferase assays were performed as previously described (2).

RT-PCR experiments. HELN-ERα, -ERβ, -ΔAB-ERα and -ΔAB-ERβ or MCF-7 cells were treated 24h with E_2 or bisphenols. RNA was extracted from the cells using the RNeasy RNA isolation kit (Qiagen). For RNA extractions, two independent cultures were performed per condition. Reverse transcription was performed with random hexamers on 1 μg of total RNA using the SuperScript II reverse transcriptase (Invitrogen) and the reaction was diluted 10 times for amplification. The mRNA levels of PR, pS2, RIP140 and GREB1 were quantified by real time-PCR quantification using a SYBR Green technology (LightCycler, Roche). Results were normalized to 28S gene and quantified using qBase.

Protein production, purification and crystallization. The human wild-type ERα LBD and the ERα-Y537S LBD mutant (amino acids 302-552) were cloned into the pET-32a vector. For both constructs, gene expression was induced in BL21(DE3) cells for 4h at 25°C in LB medium without any ligand and the protein was purified in the apo form. The cell lysate was first applied onto a nickel affinity column (HiTrap 5 mL; GE Healthcare). The eluted protein was then dialyzed in 20 mM Tris pH 8.0, 50 mM NaCl, 10 mM β-mercaptoethanol and 10% glycerol, overnight at 4°C. During dialysis, the N-terminal thioredoxine-hexahistidine tag was removed by adding thrombin to the sample (2 U per mg of protein), under gentle steering. The protein was separated from the cut tag by size exclusion chromatography (Superdex 75 HR 16/60; GE Healthcare) and then concentrated in the gel filtration buffer (20 mM Tris pH 8.0, 180 mM NaCl, 10 mM β-mercaptoethanol and 10% glycerol) and stored at -40°C. Prior to crystallization assays the ERα-Y537S LBD (final concentration = 0.15 mM) was mixed with 0.3 mM E_2, BPA or BPAF and 0.3 mM SRC-1 NR2 co-activator peptide. Co-crystals with E_2 were obtained in 200 mM Li_2SO_4, 100 mM Tris pH 8.5, 30% PEG 4000, while the BPA and BPAF complexes crystallized in 300 mM NaCl, 100 mM Hepes pH 7.75, 30-32% PEG 3350.

The wild-type ERα LBD (final concentration = 0.15 mM) was mixed with 0.3 mM BPC and crystallized in 200 mM $MgCl_2$, 100 mM BisTris pH 5.5, 25% PEG 3350.

Data collection and structure determination. For all complexes, native data were collected from one crystal cryoprotected with 30% glycerol on the ID14-1, ID23-2 or ID29 beamlines at the European Synchrotron Radiation Facility, Grenoble, France. Data were processed and scaled with XDS and XSCALE (3). Crystals belong to space group $P2_1$ for the complexes with E_2, BPA and BPAF, and to $P1$ for the complex with BPC. The X-ray structures were solved by molecular replacement method using PHENIX (phenix.automr) (4), and refinement and rebuilding were performed with COOT (5), PHENIX (phenix.refine) (4) and REFMAC (6) from the CCP4 (7) suite. Data collection and refinement statistics are summarized in Table S1. Figures were prepared with PyMOL (http://pymol.org/).

Thermal shift assays (Thermofluor®). This method is measuring protein unfolding based on fluorescence detection of the denatured form of the protein (8). Solutions of 15 µL containing 4 µM protein, 40 µM ligand and 1X Sypro® Orange in 20 mM Tris pH 8.0, 180 mM NaCl, 5 mM DTT, 10% glycerol were added to the wells of a 96-well PCR plate. DMSO was added instead of ligand in the tests for the apo forms. The plates were sealed with an optical sealing tape (Bio-Rad) and heated in an Mx3005P Q-PCR system (Stratagene) from 25 to 95°C at 1°C intervals. Fluorescence changes in the wells were monitored with a photomultiplier tube. The wavelengths for excitation and emission were 545 nm and 568 nm, respectively. The melting temperatures, Tm, were obtained by fitting the fluorescence data from two independent experiments with a Boltzmann model using the GraphPad Prism software.

Fluorescence anisotropy measurements. Measure of the binding affinities of the fluorescein-labeled SRC-1 NR2 peptide for wild-type ERα and ERα-Y537S LBDs in the absence and presence of various ligands was performed using a Safire^2 microplate reader (TECAN) with the excitation wavelength set at 470 nm and emission measured at 530 nm. Experiments were performed as previously described (9). The reported data are the average of three independent experiments and error bars correspond to standard deviations. Helix H12 dynamics was monitored using the fluorescein-labeled ERα LBD homodimer prepared following the previously described protocol (10). Briefly, wild-type ERα LBD was produced as a fusion with the intein and chitin-binding domains using the vector pTYB1 (New England Biolabs). C-terminal labeling was performed using 1 mM cystein-fluorescein with 250 mM MESNA after purification and elution from chitin resin. Excess of cystein-fluorescein was removed using a Zeba^{TM} Desalt Spin Column (Pierce). The dimeric ERα was then purified to homogeneity using size exclusion chromatography. Fluorescence anisotropy assays were performed using a Safire^2 microplate reader (TECAN) at a protein concentration of 0.140 µM. The excitation wavelength was set at 470 nm, with emission measured at 530 nm. The SRC-1 NR2 coactivator peptide was added to protein samples containing 5 µM of ligand to a final concentration of 10 µM and then the sample was diluted successively with 20 mM Tris pH 8.0, 180 mM NaCl, 5 mM DTT and 10% glycerol supplemented with 0.140 µM of protein and 5 µM of ligand. At least three independent measurements were made for each sample.

Virtual ligand screening. For all receptors studied, ERα, ERβ, ERRγ and AR, six distinct conformations were selected according to the best predicted affinities after ligand cross docking using the server @TOME-2 (11) and three implemented scoring functions: X-score (12), MEDUSASCORE (13) and DSX (14). Four cross-docked ligands in each conformation were used as shape restraint (using a weight term lowered to -2 from the default -3 value) in PLANTS (15). Orientation of side chains within a binding site are optimized during the docking by PLANTS. Virtual screening was performed with default parameters otherwise. Results are available through a Web-portal at: http://atome.cbs.cnrs.fr/EDCNR.html.

References

1. Molina-Molina JM, *et al.* (2008) Profiling of benzophenone derivatives using fish and human estrogen receptor-specific in vitro bioassays. *Toxicol Appl Pharmacol* 232(3):384-395.
2. le Maire A, *et al.* (2009) Activation of RXR-PPAR heterodimers by organotin environmental endocrine disruptors. *EMBO Rep* 10(4):367-373.
3. Kabsch W (2010) XDS. *Acta Crystallogr D Biol Crystallogr* 66:125-132.
4. Adams PD, *et al.* (2010) PHENIX: a comprehensive Python-based system for macromolecular structure solution. *Acta Crystallogr D Biol Crystallogr* 66:213-221.
5. Emsley P & Cowtan K (2004) Coot: model-building tools for molecular graphics. *Acta Crystallogr D Biol Crystallogr* 60(Pt 12 Pt 1):2126-2132.
6. Murshudov GN, Vagin AA, & Dodson EJ (1997) Refinement of Macromolecular Structures by the Maximum-Likelihood method. *Acta Crystallogr D Biol Crystallogr* 53:240-255.
7. Winn MD, *et al.* (2011) Overview of the CCP4 suite and current developments. *Acta Crystallogr D Biol Crystallogr* 67:235-242.
8. Pantoliano MW, *et al.* (2001) High-Density Miniaturized Thermal Shift Assays as a General Strategy for Drug Discovery. *J Biomol Screen* 6(6):429-440.
9. Pogenberg V, *et al.* (2005) Characterization of the interaction between retinoic acid receptor/retinoid X receptor (RAR/RXR) heterodimers and transcriptional coactivators through structural and fluorescence anisotropy studies. *J Biol Chem* 280(2):1625-1633.
10. Nahoum V, *et al.* (2007) Modulators of the structural dynamics of the retinoid X receptor to reveal receptor function. *Proc Natl Acad Sci U S A* 104(44):17323-17328.
11. Pons JL & Labesse G (2009) @TOME-2: a new pipeline for comparative modeling of protein-ligand complexes. *Nucleic Acids Res* (37 Web Server issue:W485-91).
12. Wang R, Lai L, & Wang S (2002) Further development and validation of empirical scoring functions for structure-based binding affinity prediction. *J Comput Aided Mol Des* 16(1):11-26.
13. Yin S, Biedermannova L, Vondrasek J, & Dokholyan NV (2008) MedusaScore: an accurate force field-based scoring function for virtual drug screening. *J Chem Inf Model* 48(8):1656-1662.
14. Neudert G & Klebe G (2011) DSX: A Knowledge-Based Scoring Function for the Assessment of Protein-Ligand Complexes. *J Chem Inf Model* 51(10):2731-2745.
15. Korb O, Stützle T, & Exner TE (2009) Empirical Scoring Functions for Advanced Protein-Ligand Docking with PLANTS. *J Chem Inf Model* 49(1):84-96.

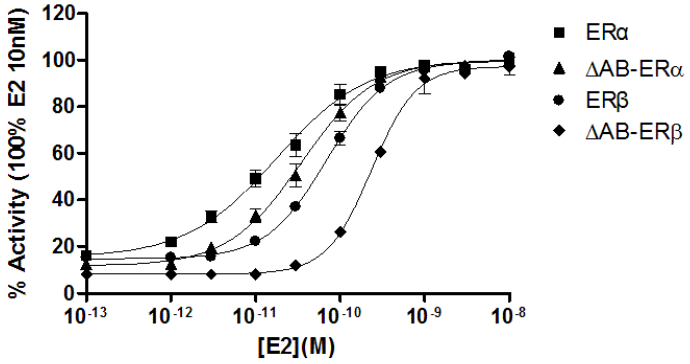

Fig.S1. Dose response curve for E_2 in reporter cell lines. HELN-ERα and -ΔAB-ERα and HELN-ERβ and -ΔAB-ERβ luciferase assays of E_2. The maximal luciferase activity (100%) was obtained with 10 nM E_2. Values were the mean ± SD from three separate experiments.

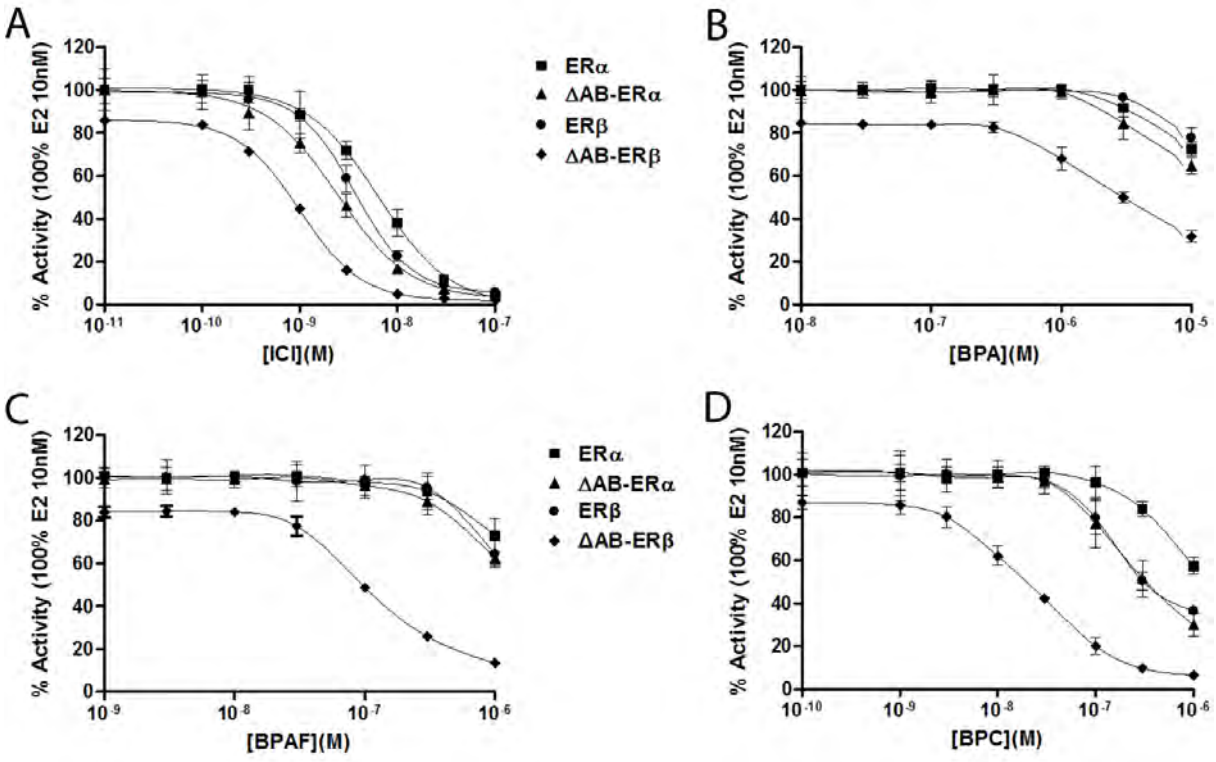

Fig.S2. (*A*) ICI-, (*B*) BPA-, (*C*) BPAF, (*D*) BPC-induced inhibition of ERα, ERβ, ΔAB-ERα, and ΔAB-ERβ activation by E_2. HELN-ERs cells were incubated with different concentrations (10 pM–10 μM) of ICI 182780 and bisphenols in the presence of 1 nM E_2. Values are the mean ± SD from three separate experiments. Note that the scale of the Y axis is different in the four graphs.

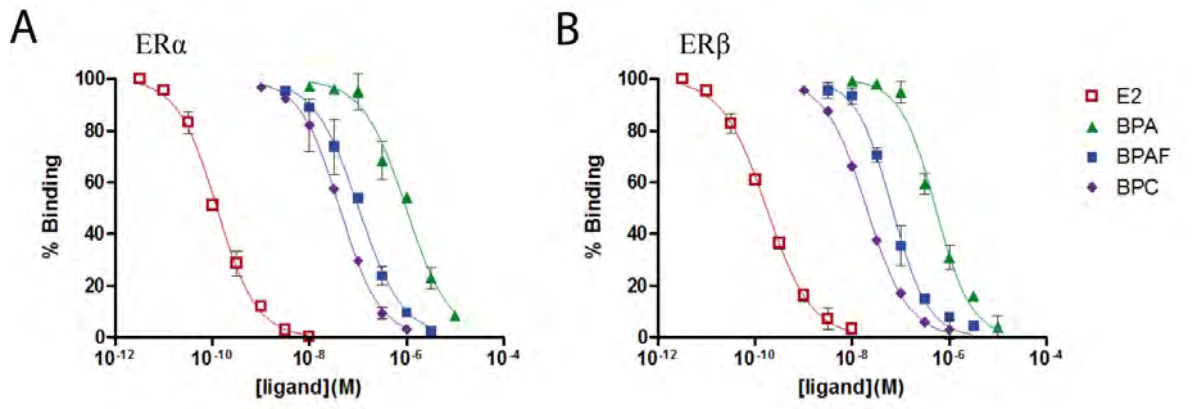

Fig.S3. Competition inhibition of [^{3}H]-E_2 binding to (*A*) ERα and (*B*) ERβ by bisphenols. HELN-ERα and -ERβ cells were incubated with different concentrations (3 pM–10 μM) of E_2, BPA, BPAF and BPC in the presence of 0.1 nM [^{3}H]-E_2. Kds are 0.124 and 0.173 nM for E_2, 984 and 523 nM for BPA, 103 and 66.5 nM for BPAF and 42.3 and 19.2 nM for BPC for ERα and ERβ respectively. Values were the mean ± SD from three separate experiments.

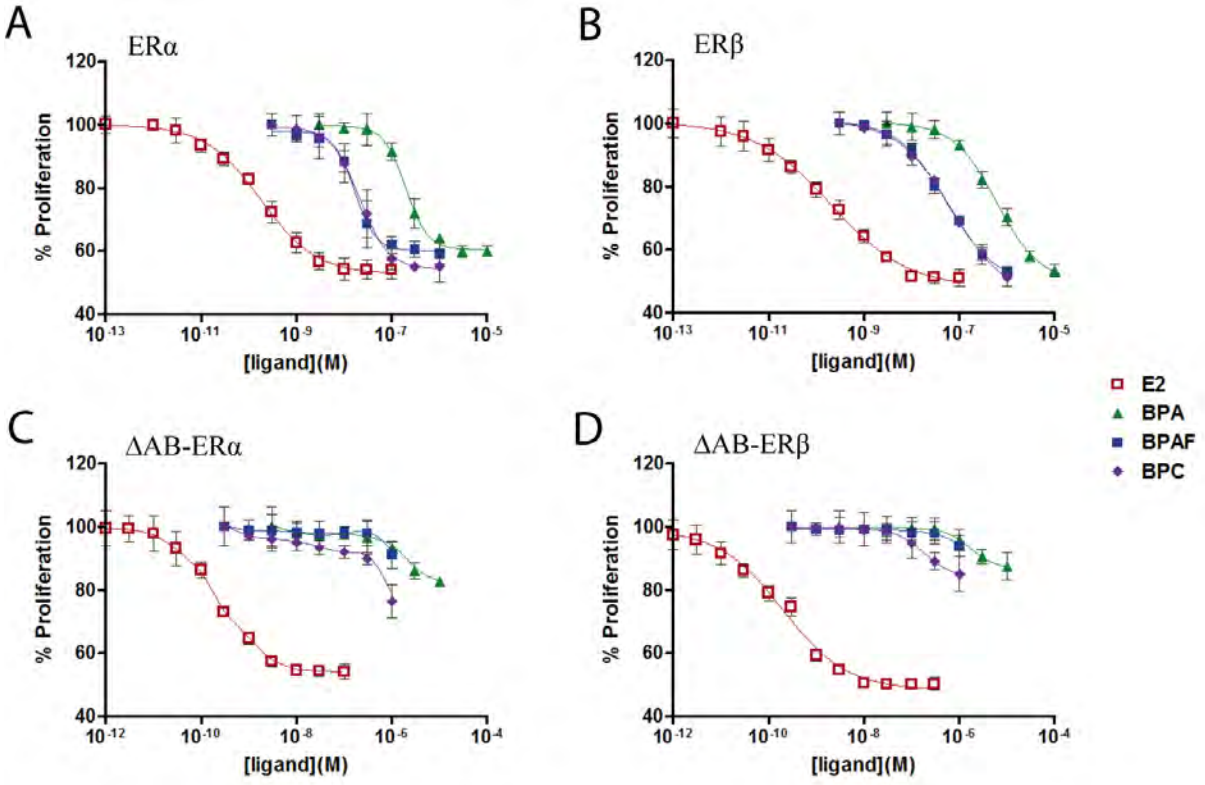

Fig.S4. Proliferative response of HELN-ER cells upon treatment with E_2 and bisphenols. (*A*, *B*) Dose response curves of BPA, BPAF and BPC using cells transfected with ERα (*A*) and ERβ (*B*). Cells were treated with indicated compounds for 10 days (with replenishment of ligands in fresh medium every 2 days) at the indicated concentrations. Data are expressed as percentage with respect to the ligand free control (100%). Values are the mean ± SD from three separate experiments. (*C*, *D*) Same experiment using cells transfected with ΔAB-ERα (*C*) and ΔAB-ERβ (*D*). Note that the scale of the Y axis is different in the four graphs.

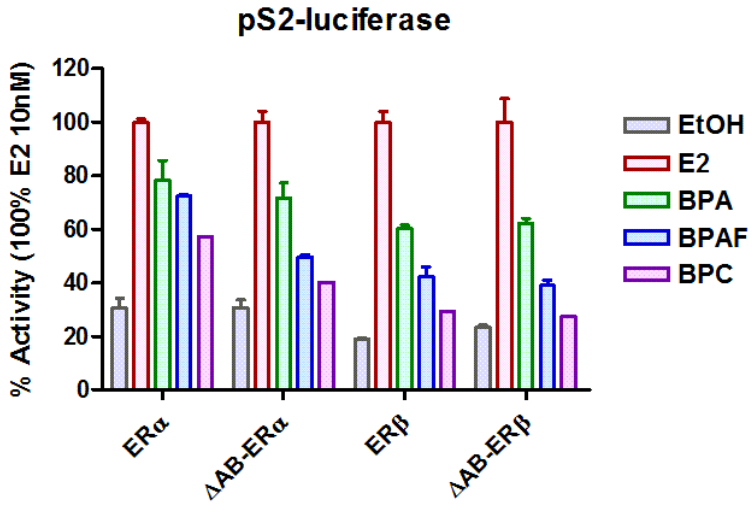

Fig.S5. The partial agonism of bisphenols is also observed on the pS2 promoter in HeLa cells. HeLa cells transiently transfected with the reporter pS2 promoter-Luciferase and pSG5-ERα, pSG5-ΔAB-ERα, pSG5-ERβ or pSG5-ΔAB-ERβ were incubated with E_2 10 nM, BPA 10 µM, BPAF and BPC 1 µM.

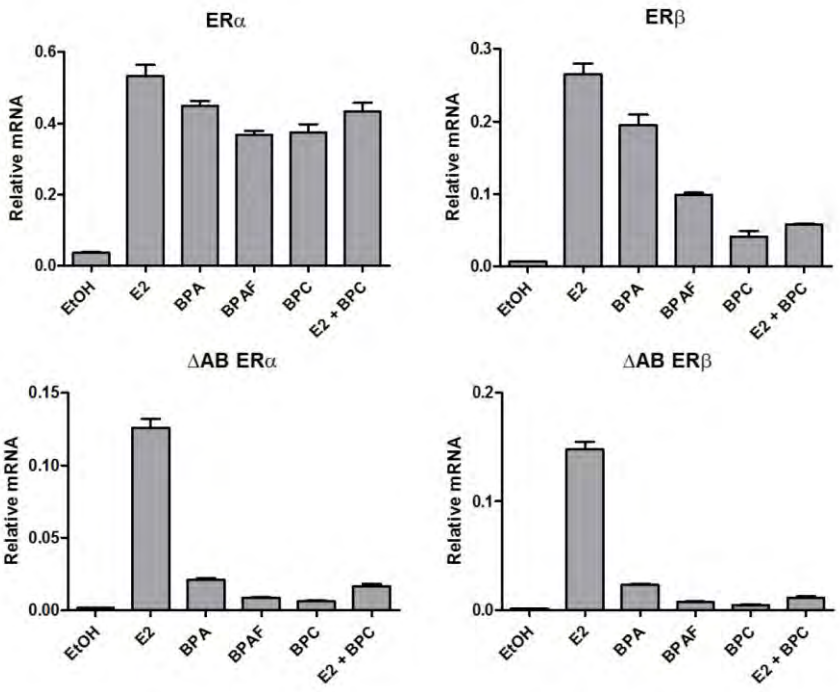

Fig.S6. In HeLa cells, bisphenols partially activated the expression of GREB1 gene. Quantitative real-time PCR (QRT-PCR) of GREB1 expression levels in HELN-ERα, -ΔAB-ERα, -ERβ or -ΔAB-ERβ cells treated with E_2 10 nM, BPA 10 µM, BPAF, BPC 1 µM and E_2 10 nM + BPC 1 µM. Data were normalized to 28s control and plotted as average of absolute gene expression levels ± SEM (n=3).

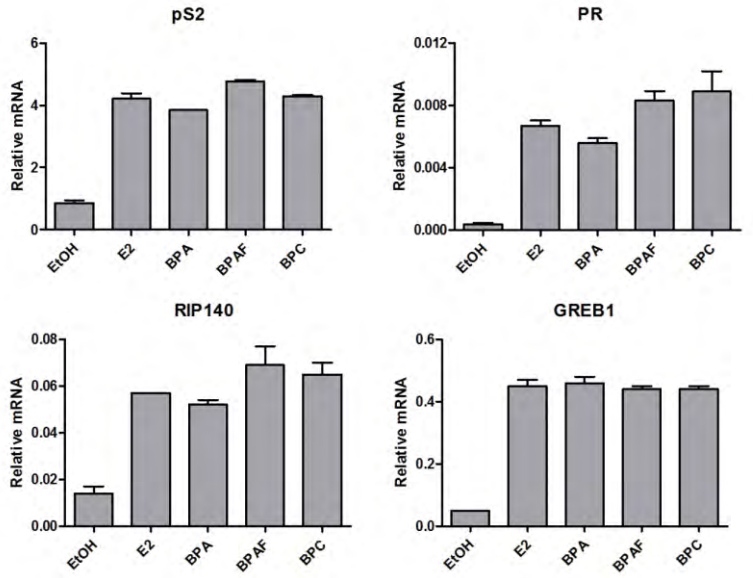

Fig.S7. In MCF-7 cells, bisphenols fully activated the expression of E_2 regulated genes. Quantitative real-time PCR (QRT-PCR) of pS2, PR, RIP140 and GREB1 expression levels in MCF-7 cells treated with E_2 10 nM, BPA 10 µM, BPAF and BPC 1 µM. Data were normalized to 28s control and plotted as average of absolute gene expression levels ± SEM (n=3).

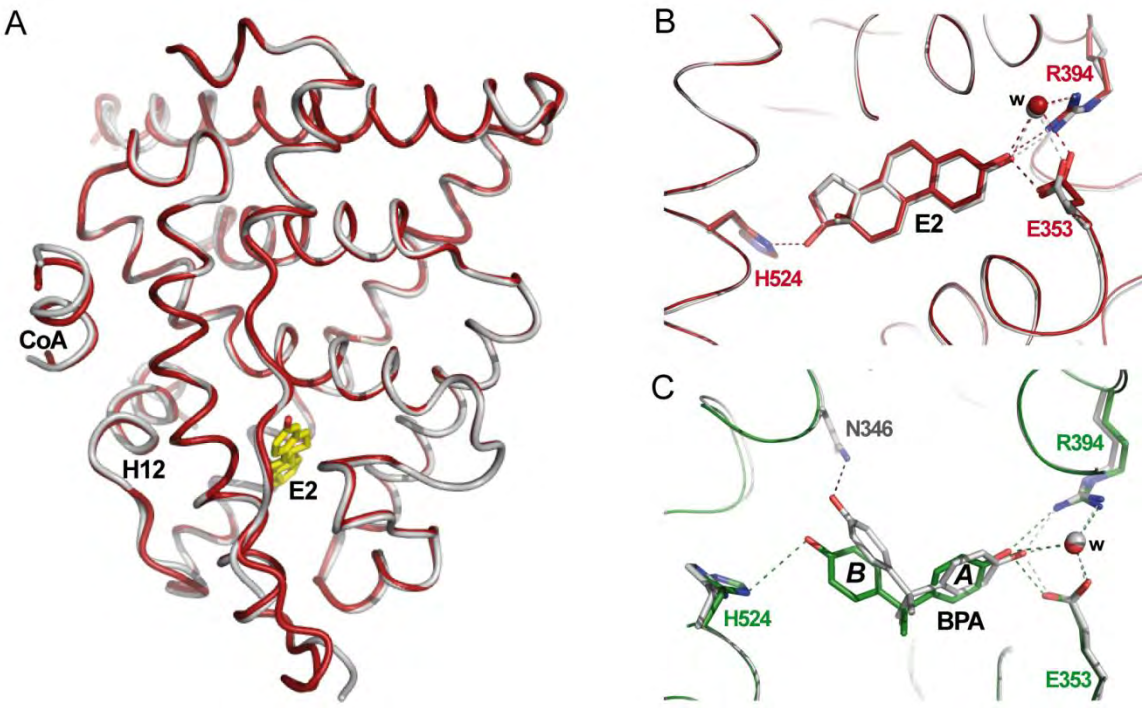

Fig.S8. Crystal structure of ERα-Y537S LBD. (*A*) The superimposition of the structure of ERα-Y537S LBD in complex with E_2 on that of the corresponding wild-type complex (PDB code 1GWR) reveals a high degree of similarity (Rmsd = 0.479 Å for 230 Cα). The wild-type receptor is shown in grey whereas the Y537S mutant is shown in red. (*B*) Close-up view of the ligand-binding pocket showing that the binding modes of E_2 are identical in the wild-type and the mutant receptors. (*C*) Superimposition of the structure of ERα-Y537S LBD on that of ERRγ LBD (PDB code 2P7G) showing the different docking modes of BPA in the two receptors. The ERα-Y537S and ERRγ LBD receptors are shown in green and grey, respectively.

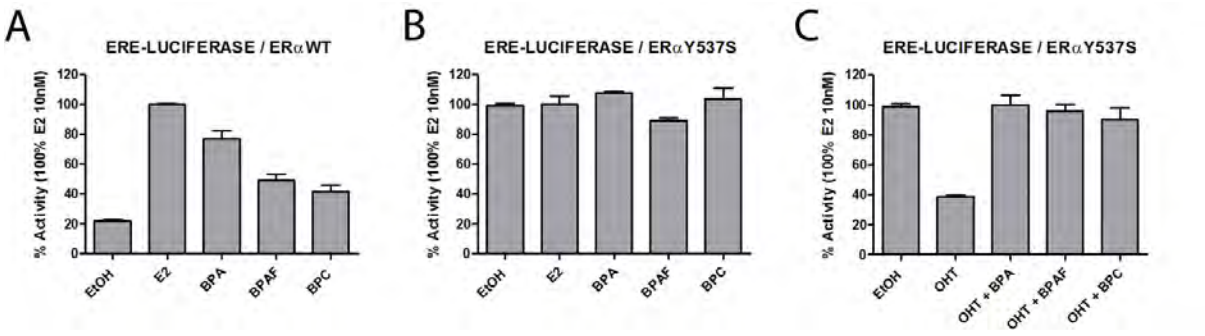

Fig.S9. ERα-Y537S has a constitutive activity which is repressed by OHT but not bisphenols. HeLa cells transiently transfected with the reporter ERE-βGlobin-Luciferase (*A*, *B*, *C*) and pSG5-ERα wild-type (*A*) or Y537S (*B*, *C*) were incubated with (*A*, *B*) E_2 10 nM, BPA 10 μM, BPAF and BPC 1 μM or (*C*) OHT 1 nM, OHT 1 nM + BPA 10 μM, OHT 1 nM + BPAF 1 μM and OHT 1 nM + BPC 1 μM.

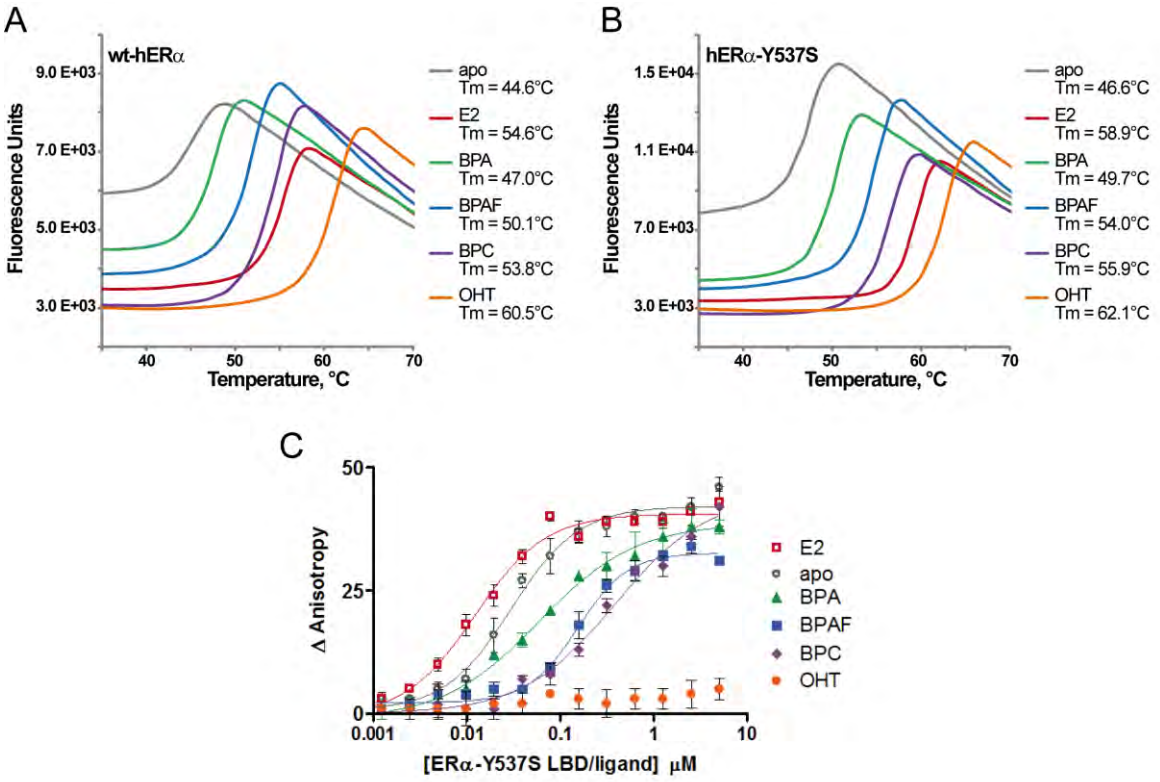

Fig.S10. Biophysical characterization of the ERα-Y537S mutant. Thermal denaturation curves of wild-type ERα (*A*) and ERα-Y537S (*B*) in the absence of ligand or in the presence of E_2, BPA, BPAF, BPC or OHT. Melting temperatures, Tm, are indicated. All ligands display a protective effect against thermal denaturation. The Y537S mutation also induces a global shift of melting temperatures indicating that it has a positive effect on the overall stability of the receptor domain. Of note, the ranking order of ligand effects (OHT>E2>BPC>BPAF>BPA>apo) is conserved in the two sets of experiments. (*C*) Titration of fluorescein-labeled SRC-1 NR2 peptide by ERα-Y537S in the absence of ligand or in the presence of E_2, OHT, BPA, BPAF or BPC. As compared with the wild-type receptor, a shift of the affinities towards lower Kd is consistent with a stabilization of the active conformation by the Y537S mutation.

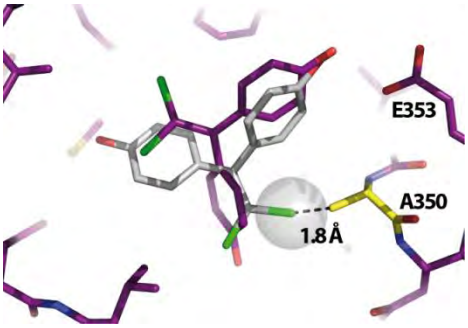

Fig.S11. Modeling of BPC in the "BPA-like" orientation (in grey) reveals a steric clash between one chlorine atom (colored in green) of BPC and the methyl group of A350 which prevents BPC from adopting this position in the ligand-binding pocket. The sphere represents the van der Waals radius of the chlorine atom (1.75 Å). The crystal structure of the complex with BPC is shown in purple.

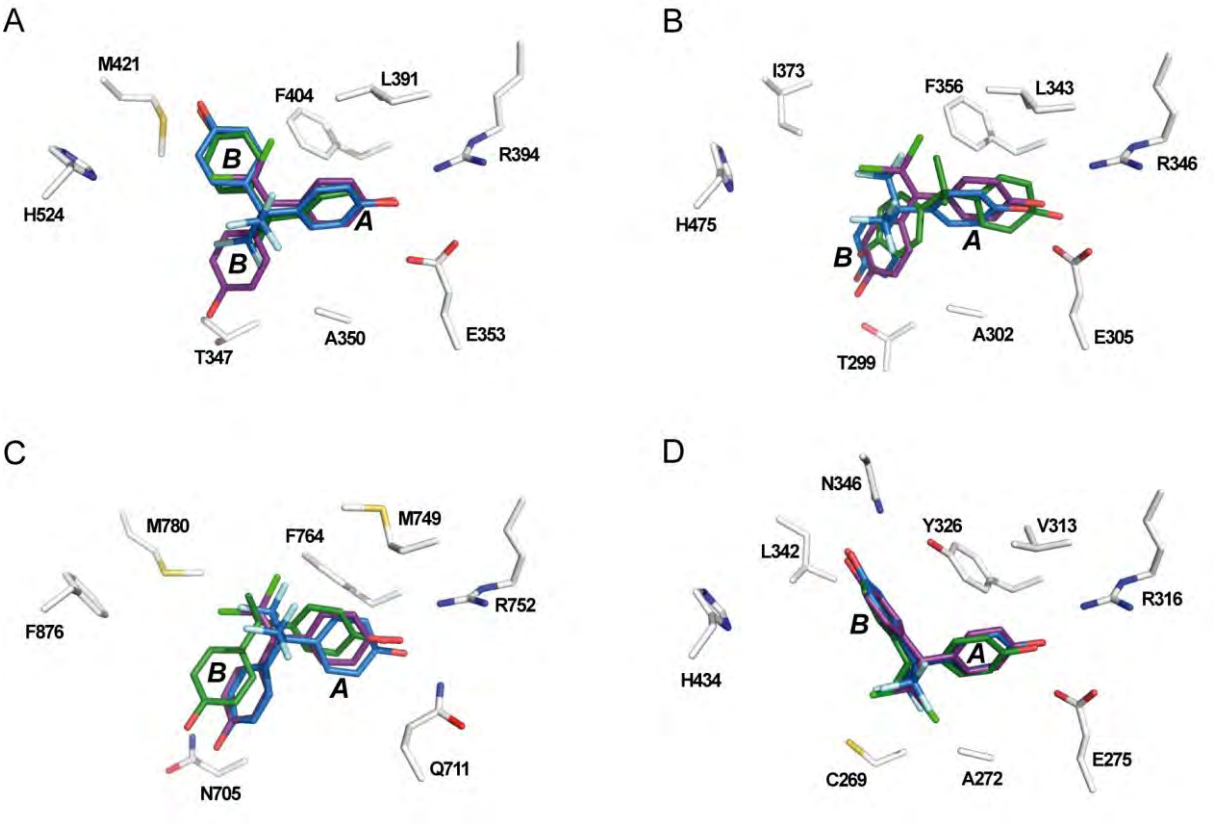

Fig.S12. Predicted orientation of bisphenols found by virtual screening. BPA, BPAF and BPC are shown in green, blue and purple, respectively. While BPA and BPAF adopt the BPA-like orientation and the BPC the BPC-like orientation in ERα (*A*), these three bisphenols are predicted to adopt the BPC-like orientation in ERβ (*B*) and AR (*C*), and the BPA-like orientation in ERRγ (*D*). The interaction of phenol ring A with E353 and R394, or equivalent residues, is conserved in all four receptors. The phenol ring B is predicted to interact with T299 in ERβ (*B*), N705 in AR (*C*) or N346 in ERRγ (*D*).

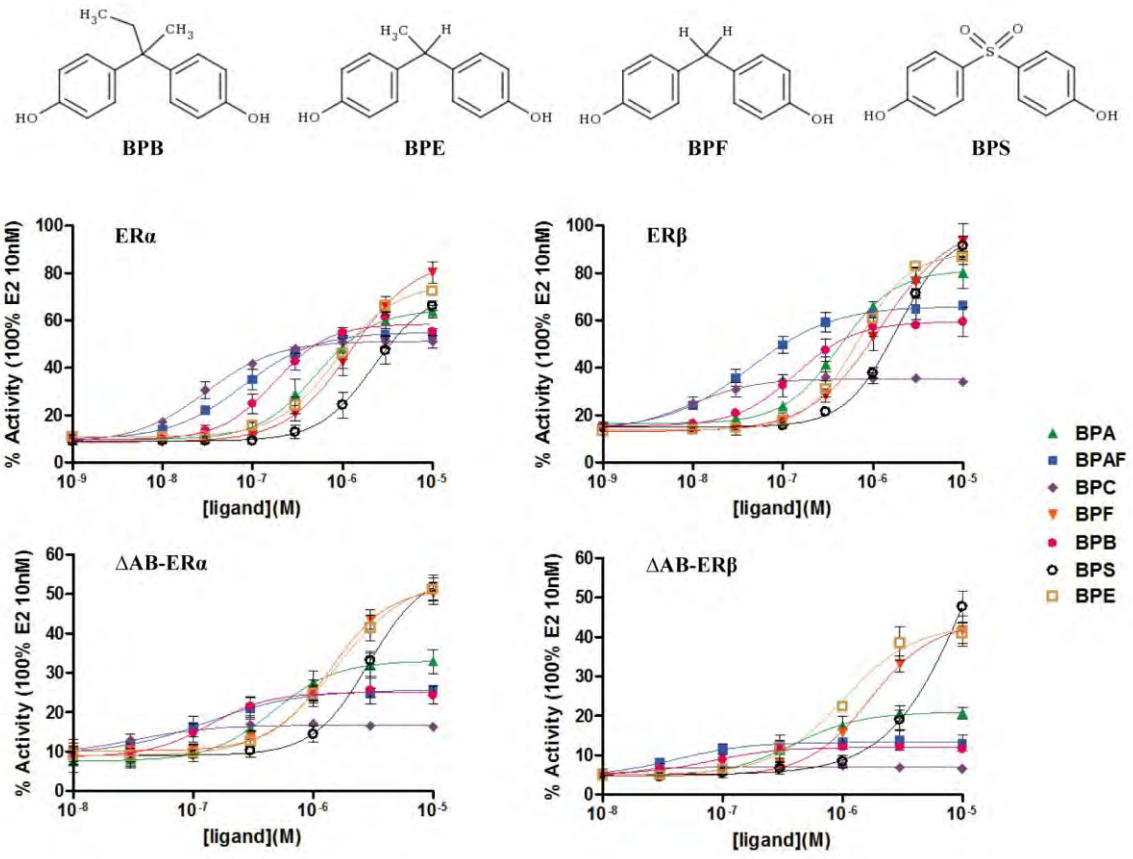

Fig.S13. Bisphenol-induced activation of ERs. HELN-ERα, -ERβ, -ΔAB-ERα and -ΔAB-ERβ cells were incubated with different concentrations (0.001–10 μM) of bisphenols. The maximal luciferase activity (100%) was obtained with 10 nM E_2. Values were the mean ± SD from three separate experiments. Note that the scale of the Y axis is different in the four graphs.

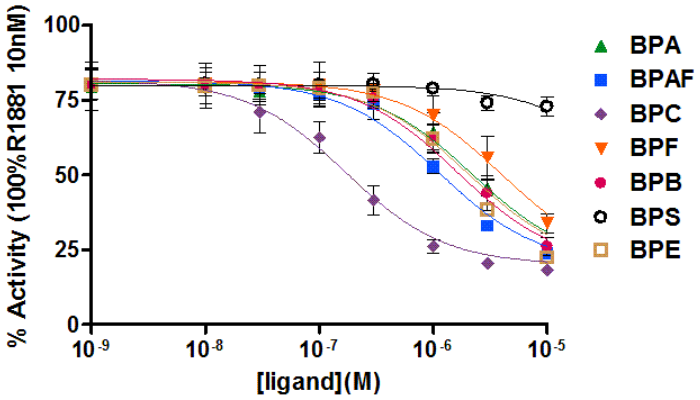

Fig.S14. Bisphenol-induced inhibition of AR activation by R1881. HELN-AR (ERα DBD) cells were incubated with different concentrations of bisphenols in the presence of 1 nM R1881. The maximal luciferase activity (100%) was obtained with 10 nM R1881. Values were the mean ± SD from three separate experiments. Derived Kis are: BPA 2.65 µM, BPAF 1.34 µM, BPC 0.19 µM, BPF 3.95 µM, BPS not determined, BPB 2.24 µM and BPE 1.6 µM.

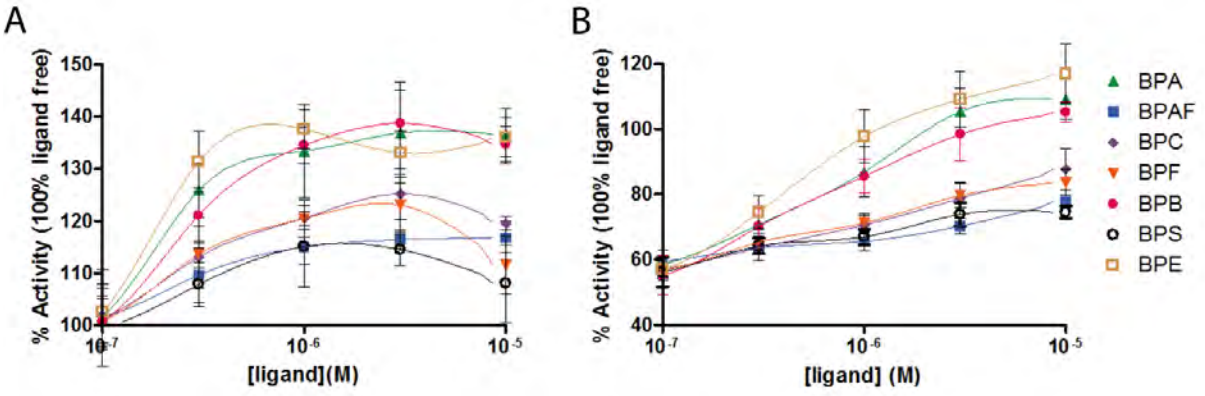

Fig.S15. Bisphenol-induced activation of ERRγ. (A) HG5LN GAL4-ERRγ cells were incubated with different concentrations of bisphenols. (B) HG5LN GAL4-ERRγ cells were incubated with different concentrations of bisphenols in the presence of 1 µM OHT. Data are expressed as percentage with respect to the ligand free control (100%). Values were the mean ± SD from three separate experiments.

Table S1. Data collection and refinement statistics

	E_2-3UUD	BPA-3UU7	BPAF-3UUA	BPC-3UUC
Data collection				
Space group	$P\,2_1$	$P\,2_1$	$P\,2_1$	$P\,1$
Cell dimensions				
a, Å	56.23	54.85	54.70	53.53
b, Å	82.02	81.58	81.95	58.64
c, Å	58.93	58.52	58.88	93.02
α, °	90.00	90.00	90.00	75.64
β, °	111.06	110.68	110.74	74.77
γ, °	90.00	90.00	90.00	62.82
Resolution, Å	45.68 – 1.60 (1.69 – 1.60)*	46.53 – 2.20 (2.33 – 2.20)*	46.60 – 2.05 (2.17 – 2.05)*	46.88 – 2.10 (2.15 – 2.10)*
R_{sym}, %	3.9 (47.0)	10.6 (43.2)	5.2 (47.5)	4.8 (42.1)
$I/\sigma I$	18.2 (2.5)	8.4 (3.0)	15.1 (2.7)	10.5 (1.8)
Completeness, %	99.5 (99.8)	99.5 (99.2)	99.3 (99.5)	91.4 (90.4)
Redundancy	3.7 (3.7)	3.8 (3.8)	3.7 (3.6)	1.8 (1.8)
Refinement				
Resolution, Å	45.68 – 1.60	46.53 – 2.20	46.60 – 2.05	46.88 – 2.10
No. of reflections	65,563	24,610	30,405	51,238
R/R_{free}	0.166 / 0.195	0.206 / 0.245	0.189 / 0.231	0.214 / 0.255
$B_{factors}$, Å^2				
All	28.1	34.3	46.5	34.2
Protein	27.1	34.3	46.5	34.1
Ligands	16.8	33.1	52.7	33.6
Water	38.2	34.0	45.6	37.4
Rmsd				
Bond lengths, Å	0.008	0.005	0.004	0.007
Bond angles, °	1.021	0.616	0.762	0.891

*The values in parentheses are for the highest-resolution shell.